University of Pretoria etd – Labuschagne, A (2006)

Chapter 6

Vertical slender structure

6.1 Introduction

Newland claims in [N2] that the inclusion of a resilient seating increases the complexity of a finite element analysis. However, in the way that we model the resilient seating, the application of the finite element method doesn't become more complicated. It involves only the introduction of some extra variables. The effect is, that in comparison with the models for a rigid base, the inertia, bending and damping matrices slightly increase in size and the entries of the mentioned matrices change at only a few entries.

We show in this chapter how to implement the finite element method for approximating the eigenvalues for Problems VR 4 and VT 4. Results are compared to results in [LVV].

We also study the effect of the "gravity"-term described in Chapter 2 by Equations (2.1.4) and (2.1.17), i.e. the constitutive equation

$$L(x,t) = \mu(1-x)\partial_x w(x,t).$$

University of Pretoria etd – Labuschagne, A (2006)

6.2 The eigenvalue problem

6.2.1 The Rayleigh model

For the modal analysis of the system, $\tilde{w}(x,t) = e^{\lambda t}w(x)$ is considered as a possible solution. For the two different models under consideration (models 3 and 4), the additional variables are handled in a similar way as for w, as can be seen below. This requires consideration of the corresponding eigenvalue problems.

For Problem VR 3, we consider $\tilde{\theta}_F(t) = e^{\lambda t}\theta_F$ as a possible solution.

Variational form for Problem VRE 3

Find w and θ_F such that $w \in T(0,1)$,

$$\begin{aligned}\lambda^2 c_A(w,v) + b_A(w,v) + \lambda C_F w(0)v(0) - k\theta_F v'(0)\\ +\lambda c\Big(w'(0) - \theta_F\Big)v'(0) \;=\; 0\end{aligned} \tag{6.2.1}$$

holds for each $v \in T(0,1)$ and

$$\begin{aligned}\lambda^2 I_F\theta_F - k\Big(w'(0) - \theta_F\Big) - \lambda c\Big(w'(0) - \theta_F\Big)\\ +k_F\theta_F + \lambda c_F\theta_F \;=\; 0.\end{aligned} \tag{6.2.2}$$

For Problem VR 4 consider the following possible solutions.

$$\tilde{w}_F(t) = e^{\lambda t}w_F, \quad \tilde{\theta}_B(t) = e^{\lambda t}\theta_B \quad \text{and} \quad \tilde{\theta}_F(t) = e^{\lambda t}\theta_F.$$

Variational form for Problem VRE 4

Find w, w_F, θ_B and θ_F such that $w \in T(0,1)$,

$$\begin{aligned}\lambda^2 c_A(w,v) + b_A(w,v) - K_{FB}w_F v(0) + \lambda C_{FB}\Big(w(0) - w_F\Big)v(0)\\ +\lambda c_{BA}\Big(w'(0) - \theta_B\Big)v'(0) - k_{BA}\theta_B v'(0) \;=\; 0\end{aligned} \tag{6.2.3}$$

University of Pretoria etd – Labuschagne, A (2006)

holds for each $v \in T(0,1)$ and

$$\begin{aligned}\lambda^2 I_B\theta_B - k_{BA}\Big(w'(0)-\theta_B\Big) - \lambda c_{BA}\Big(w'(0)-\theta_B\Big)\\ +k_{FB}\Big(\theta_B-\theta_F\Big) + \lambda c_{FB}\Big(\theta_B-\theta_F\Big) \;=\; 0,\end{aligned} \tag{6.2.4}$$

$$\begin{aligned}\lambda^2 m_F w_F - K_{FB}\Big(w(0)-w_F\Big) - \lambda C_{FB}\Big(w(0)-w_F\Big)\\ +K_F w_F + \lambda C_F w_F \;=\; 0,\end{aligned} \tag{6.2.5}$$

$$\begin{aligned}\lambda^2 I_F\theta_F - k_{FB}\Big(\theta_B-\theta_F\Big) - \lambda c_{FB}\Big(\theta_B-\theta_F\Big)\\ +k_F\theta_F + \lambda c_F\theta_F \;=\; 0.\end{aligned} \tag{6.2.6}$$

Remark

Note that the bilinear forms used in the formulation above, are the bilinear forms defined for the variational form and not the weak variational form.

6.2.2 The Timoshenko model

Here we consider $\tilde{w}(x,t) = e^{\lambda t}w(x)$ and $\tilde{\phi}(x,t) = e^{\lambda t}\phi(x)$ as possible solutions and follow the same approach as in the Rayleigh models to formulate Problems VTE 3 and VTE 4.

We consider $\tilde{\theta}_F(t) = e^{\lambda t}\theta_F$ as a possible solution for Problem VT 3.

Problem VTE 3

Find w, ϕ and θ_F such that $w \in T(0,1)$ and $\phi \in T(0,1)$,

$$\begin{aligned}\lambda^2(w,v) + \lambda^2 m_F w(0)v(0) + (w'-\phi,v') + K_F w(0)v(0)\\ +\lambda C_F w(0)v(0) \;=\; 0\end{aligned} \tag{6.2.7}$$

holds for each $v \in T(0,1)$,

$$\begin{aligned}\frac{\lambda^2}{\alpha}\,(\phi,\psi) + \frac{1}{\beta}\,(\phi',\psi') - (w'-\phi,\psi) - \mu\int_0^1 (1-x)w'(x)\psi(x)\,dx\\ +k\Big(\phi(0)-\theta_F\Big)\psi(0) + \lambda c\Big(\phi(0)-\theta_F\Big)\psi(0) \;=\; 0,\end{aligned} \tag{6.2.8}$$

University of Pretoria etd – Labuschagne, A (2006)

holds for each $\psi \in T(0,1)$ and

$$\begin{aligned}\lambda^2 I_F\theta_F - k\Big(\phi(0)-\theta_F\Big) - \lambda c\Big(\phi(0)-\theta_F\Big)\\ +k_F\theta_F + \lambda c_F\theta_F \;=\; 0.\end{aligned} \tag{6.2.9}$$

For Problem VT 4, consider the following possible solutions.

$$\tilde{w}_F(t) = e^{\lambda t}w_F, \quad \tilde{\theta}_B(t) = e^{\lambda t}\theta_B \quad \text{and} \quad \tilde{\theta}_F(t) = e^{\lambda t}\theta_F.$$

Variational form for Problem VTE 4

Find w, ϕ, w_F, θ_B and θ_F such that $w \in T(0,1)$ and $\phi \in T(0,1)$,

$$\begin{aligned}\lambda^2(w,v) + \lambda^2 m_B w(0)v(0) + (w'-\phi, v') + K_{FB}\Big(w(0)-w_F\Big)v(0)\\ +\lambda C_{FB}\Big(w(0)-w_F\Big)v(0) \;=\; 0\end{aligned} \tag{6.2.10}$$

holds for each $v \in T(0,1)$,

$$\begin{aligned}\frac{\lambda^2}{\alpha}\,(\phi,\psi) + \frac{1}{\beta}\,(\phi',\psi') - (w'-\phi,\psi) - \mu\int_0^1 (1-x)w'(x)\psi(x)\,dx\\ +k_{BA}\Big(\phi(0)-\theta_B\Big)\psi(0) + \lambda c_{BA}\Big(\phi(0)-\theta_B\Big)\psi(0) = 0\end{aligned} \tag{6.2.11}$$

holds for each $\psi \in T(0,1)$ and

$$\begin{aligned}\lambda^2 I_B\theta_B - k_{BA}\Big(\phi(0)-\theta_B\Big) - \lambda c_{BA}\Big(\phi(0)-\theta_B\Big)\\ +k_{FB}\Big(\theta_B-\theta_F\Big) + \lambda c_{FB}\Big(\theta_B-\theta_F\Big) \;=\; 0,\end{aligned} \tag{6.2.12}$$

$$\begin{aligned}\lambda^2 m_F w_F - K_{FB}\Big(w(0)-w_F\Big) - \lambda C_{FB}\Big(w(0)-w_F\Big)\\ +K_F w_F + \lambda C_F w_F \;=\; 0,\end{aligned} \tag{6.2.13}$$

$$\begin{aligned}\lambda^2 I_F\theta_F - k_{FB}\Big(\theta_B-\theta_F\Big) - \lambda c_{FB}\Big(\theta_B-\theta_F\Big)\\ +k_F\theta_F + \lambda c_F\theta_F \;=\; 0.\end{aligned} \tag{6.2.14}$$

University of Pretoria etd – Labuschagne, A (2006)

6.3 Galerkin approximations for the eigenvalue problem

6.3.1 Rayleigh models

The interval $[0, 1]$ is divided in n subintervals of the same length. The approximate solution is denoted by w^h and written in terms of cubic basis functions δ_j as

$$w^h(x) = \sum_{j=1}^{2n+2} \delta_j(x)\, w_j\,.$$

For Problem VRE 3, substitute w^h into the variational form given by Equations (6.2.1) and (6.2.2) and take $v = \delta_i$ for $i = 1,\ 2,\ \ldots,\ 2n{+}2$. This results in the following eigenvalue problem, with θ_F as an additional unknown.

Galerkin approximation for Problem VRE 3

$$\lambda^2 \sum_{j=1}^{2n+2} c_A(\delta_j, \delta_i) w_j + \sum_{j=1}^{2n+2} b_A(\delta_j, \delta_i) w_j + \lambda C_F w_1 \delta_i(0) - k\,\theta_F\,\delta_i'(0) + \lambda c\Big(w_{n+2} - \theta_F\Big)\delta_i'(0) = 0, \tag{6.3.1}$$

$$\lambda^2 I_F \theta_F - k\Big(w_{n+2} - \theta_F\Big) - \lambda c\Big(w_{n+2} - \theta_F\Big) + k_F\theta_F + \lambda c_F \theta_F = 0. \tag{6.3.2}$$

Equations (6.3.1) and (6.3.2) describe an eigenvalue problem for which the relevant matrices are $(2n + 3) \times (2n + 3)$ matrices.

The explicit appearance of w_1 and w_{n+2} in these equations are due to the fact that $\delta_i(0) = 0$ unless $i = 1$ and $\delta_i'(0) = 0$ unless $i = n + 2$.

The same procedure is followed as for Problem VRE 3, using Equations (6.2.3) – (6.2.6). This yields a $(2n + 5) \times (2n + 5)$ eigenvalue problem, with θ_B, w_F and θ_F as three extra unknowns.

University of Pretoria etd – Labuschagne, A (2006)

Galerkin approximation for Problem VRE 4

$$\lambda^2 \sum_{j=1}^{2n+2} c_A(\delta_j, \delta_i) w_j + \sum_{j=1}^{2n+2} b_A(\delta_j, \delta_i) w_j - K_{FB} w_F \delta_i(0) + \lambda C_{FB}\Big(w_1 - w_F\Big)\delta_i(0) + \lambda c_{BA}\Big(w_{n+2} - \theta_B\Big)\delta_i'(0) - k_{BA}\theta_B \delta_i'(0) = 0, \tag{6.3.3}$$

$$\lambda^2 I_B \theta_B - k_{BA}\Big(w_{n+2} - \theta_B\Big) - \lambda c_{BA}\Big(w_{n+2} - \theta_B\Big) + k_{FB}\Big(\theta_B - \theta_F\Big) + \lambda c_{FB}\Big(\theta_B - \theta_F\Big) = 0, \tag{6.3.4}$$

$$\lambda^2 m_F w_F - K_{FB}\Big(w_1 - w_F\Big) - \lambda C_{FB}\Big(w_1 - w_F\Big) + K_F w_F + \lambda C_F w_F = 0, \tag{6.3.5}$$

$$\lambda^2 I_F \theta_F - k_{FB}\Big(\theta_B - \theta_F\Big) - \lambda c_{FB}\Big(\theta_B - \theta_F\Big) + k_F \theta_F + \lambda c_F \theta_F = 0. \tag{6.3.6}$$

6.3.2 Timoshenko models

The interval $[0, 1]$ is divided in n subintervals of the same length. The approximate solutions are denoted by w^h and ϕ^h. Written in terms of the basis functions we have

$$w^h(x) = \sum_{j=1}^{2n+2} \delta_j(x)\, w_j \quad \text{and} \quad \phi^h(x) = \sum_{j=1}^{2n+2} \delta_j(x)\, \phi_j\,.$$

Following the same line of reasoning as in the Rayleigh models, we substitute w^h and ϕ^h into the variational form equations, Equations (6.2.7) – (6.2.9). Furthermore, we let $v = \delta_i$ and $\psi = \delta_i$ for $i = 1, 2, \ldots, 2n + 2$. This yields the following $(4n + 5) \times (4n + 5)$ eigenvalue problem.

University of Pretoria etd – Labuschagne, A (2006)

Galerkin approximation for Problem VTE 3

$$\lambda^2 \sum_{j=1}^{2n+2} (\delta_j, \delta_i) w_j + \lambda^2 m_F w_1 \delta_i(0) + \sum_{j=1}^{2n+2} (\delta_j', \delta_i') w_j$$
$$- \sum_{j=1}^{2n+2} (\delta_j, \delta_i') \phi_j + K_F w_1 \delta_i(0) + \lambda C_F w_1 \delta_i(0) = 0, \qquad (6.3.7)$$

$$\frac{\lambda^2}{\alpha} \sum_{j=1}^{2n+2} (\delta_j, \delta_i) \phi_j + \frac{1}{\beta} \sum_{j=1}^{2n+2} (\delta_j', \delta_i') \phi_j - \sum_{j=1}^{2n+2} (\delta_j', \delta_i) w_j$$
$$+ \sum_{j=1}^{2n+2} (\delta_j, \delta_i) \phi_j - \mu \sum_{j=1}^{2n+2} \Big(\int_0^1 (1-x) \delta_j'(x) \delta_i(x)\, dx \Big) w_j$$
$$+ k\Big(\phi_1 - \theta_F\Big) \delta_i(0) + \lambda c \Big(\phi_1 - \theta_F\Big) \delta_i(0) = 0, \qquad (6.3.8)$$

$$\lambda^2 I_F \theta_F - k\Big(\phi_1 - \theta_F\Big) - \lambda c \Big(\phi_1 - \theta_F\Big) + k_F \theta_F + \lambda c_F \theta_F = 0. \qquad (6.3.9)$$

University of Pretoria etd – Labuschagne, A (2006)

Substituting w^h and ϕ^h into the variational form (6.2.10) – (6.2.14) and taking $v = \delta_i$ and $\psi = \delta_i$ for $i = 1, 2, \ldots, 2n+2$, the following eigenvalue problem is found.

Galerkin approximation for Problem VTE 4

$$\lambda^2 \sum_{j=1}^{2n+2} (\delta_j, \delta_i) w_j + \lambda^2 m_B w_1 \delta_i(0) + \sum_{j=1}^{2n+2} (\delta_j', \delta_i') w_j - \sum_{j=1}^{2n+2} (\delta_j, \delta_i') \phi_j + K_{FB}\Big(w_1 - w_F\Big)\delta_i(0) + \lambda C_{FB}\Big(w_1 - w_F\Big)\delta_i(0) = 0, \tag{6.3.10}$$

$$\frac{\lambda^2}{\alpha} \sum_{j=1}^{2n+2} (\delta_j, \delta_i)\phi_j + \frac{1}{\beta} \sum_{j=1}^{2n+2} (\delta_j', \delta_i')\phi_j - \sum_{j=1}^{2n+2} (\delta_j', \delta_i) w_j + \sum_{j=1}^{2n+2} (\delta_j, \delta_i)\phi_j - \mu \sum_{j=1}^{2n+2} \Big(\int_0^1 (1-x)\delta_j'(x)\delta_i(x)\, dx \Big) w_j + k_{BA}\Big(\phi_1 - \theta_B\Big)\delta_i(0) + \lambda c_{BA}\Big(\phi_1 - \theta_B\Big)\delta_i(0) = 0, \tag{6.3.11}$$

$$\lambda^2 I_B \theta_B - k_{BA}\Big(\phi_1 - \theta_B\Big) - \lambda c_{BA}\Big(\phi_1 - \theta_B\Big) + k_{FB}\Big(\theta_B - \theta_F\Big) + \lambda c_{FB}\Big(\theta_B - \theta_F\Big) = 0, \tag{6.3.12}$$

$$\lambda^2 m_F w_F - K_{FB}\Big(w_1 - w_F\Big) - \lambda C_{FB}\Big(w_1 - w_F\Big) + K_F w_F + \lambda C_F w_F = 0, \tag{6.3.13}$$

$$\lambda^2 I_F \theta_F - k_{FB}\Big(\theta_B - \theta_F\Big) - \lambda c_{FB}\Big(\theta_B - \theta_F\Big) + k_F \theta_F + \lambda c_F \theta_F = 0. \tag{6.3.14}$$

Equations (6.3.10) – (6.3.14) form a $(4n + 7) \times (4n + 7)$ system of linear equations.

University of Pretoria etd – Labuschagne, A (2006)

6.4 Matrix form of the semi-discrete problem

All four eigenvalue problems result in a quadratic eigenvalue problem of the form

$$\Big(\lambda^2\mathcal{M} + \lambda\mathcal{D} + \mathcal{K}\Big)\boldsymbol{w} = \mathbf{0}.$$

The inertia matrix $\mathcal{M}$, the bending matrix $\mathcal{K}$ and the matrix $\mathcal{D}$ due to damping are found from the variational forms for the problems. The construction of the matrices is described below.

6.4.1 The Rayleigh models

Define the $(2n+2)\times(2n+2)$ matrices M and K by

$$M_{ij} = c_A(\delta_j, \delta_i) \quad \text{and} \quad K_{ij} = b_A(\delta_j, \delta_i)\,.$$

Problem VRE 3

Let $\theta_F = w_{2n+3}$ and define

$$\boldsymbol{w} = [w_1 \; w_2 \; \cdots \; w_{2n+2} \; w_{2n+3}]^{\,T}$$

where "T" denotes the transpose of a matrix.

Let O be the $1\times(2n+2)$ zero matrix and V a $1\times(2n+2)$ matrix with all zero entries except for $V_{1,n+2} = -k$. Then

$$\mathcal{M} = \begin{bmatrix} M & O^T \\ O & I_F \end{bmatrix} \quad \text{and} \quad \mathcal{K} = \begin{bmatrix} K & V^T \\ V & (k+k_F) \end{bmatrix}.$$

Define the matrix $D^{(1)}$ as the $(n+1)\times(n+1)$ matrix with zeros everywhere except for entry $(1,1)$, for which $D^{(1)}_{11} = C_F$.

Define $D^{(2)}$ as the $(n+2)\times(n+2)$ matrix with zero entries except for $D^{(2)}_{11} = c$, $D^{(2)}_{1,n+2} = D^{(2)}_{n+2,1} = -c$ and $D^{(2)}_{n+2,n+2} = c + c_F$.

Let O be the zero matrix of size $(n+2)\times(n+1)$. Then

$$\mathcal{D} = \begin{bmatrix} D^{(1)} & O^T \\ O & D^{(2)} \end{bmatrix}.$$

University of Pretoria etd – Labuschagne, A (2006)

Problem VRE 4

Let $\theta_B = w_{2n+3}$, $w_F = w_{2n+4}$, $\theta_F = w_{2n+5}$ and define

$$\boldsymbol{w} = [w_1 \; w_2 \; \cdots \; w_{2n+4} \; w_{2n+5}]^{\,T}.$$

O is the zero $3 \times (2n+2)$ matrix and $K^{(1)}$ a $3 \times (2n+2)$ matrix with zeros entries except for $K^{(1)}_{1,n+2} = -k_{BA}$ and $K^{(1)}_{21} = -K_{FB}$.

The following matrices are defined for the damping matrix:

A $(2n+2) \times (2n+2)$ matrix $D^{(1)}$ and a $3 \times (2n+2)$ matrix $D^{(2)}$ with zero entries except for the following values:

$$D^{(1)}_{11} = C_{FB}, \quad D^{(1)}_{n+2,n+2} = c_{BA}, \quad D^{(2)}_{1,n+2} = -c_{BA} \quad \text{and} \quad D^{(2)}_{21} = -C_{FB}\,.$$

Let

$$M^{(1)} = \begin{bmatrix} I_B & 0 & \\ 0 & m_F & 0 \\ 0 & 0 & I_F \end{bmatrix}, \quad K^{(2)} = \begin{bmatrix} (k_{BA}+k_{FB}) & 0 & -k_{FB} \\ 0 & (K_{FB}+K_F) & 0 \\ -k_{FB} & 0 & (k_{FB}+k_F) \end{bmatrix}$$

$$\text{and} \quad D^{(3)} = \begin{bmatrix} (c_{BA}+c_{FB}) & 0 & -c_{FB} \\ 0 & (C_{FB}+C_F) & 0 \\ -c_{FB} & 0 & (c_{FB}+c_F) \end{bmatrix}.$$

Then

$$\mathcal{M} = \begin{bmatrix} M & O^T \\ O & M^{(1)} \end{bmatrix}, \quad \mathcal{K} = \begin{bmatrix} K & \left(K^{(1)}\right)^T \\ K^{(1)} & K^{(2)} \end{bmatrix} \quad \text{and} \quad \mathcal{D} = \begin{bmatrix} D^{(1)} & \left(D^{(2)}\right)^T \\ D^{(2)} & D^{(3)} \end{bmatrix}.$$

6.4.2 The Timoshenko models

The ij-th entry for the $(2n+2) \times (2n+2)$ matrices K, L, M and P are defined by

$$K_{ij} = (\delta'_j, \delta'_i), \quad L_{ij} = (\delta_j, \delta'_i), \quad M_{ij} = (\delta_j, \delta_i) \quad \text{and}$$

$$P_{ij} = \int_0^1 (1-x)\delta'_j(x)\delta_i(x)\,dx.$$

University of Pretoria etd – Labuschagne, A (2006)

Problem VTE 3

Define

$$\boldsymbol{w} = [w_1 \ w_2 \ \cdots \ w_{2n+2}]^{\ T} \quad \text{and} \quad \boldsymbol{\phi} = [\phi_1 \ \phi_2 \ \cdots \ \phi_{2n+2}]^{\ T}.$$

Define $\boldsymbol{z}$ in terms of the unknowns $\boldsymbol{w}$, $\boldsymbol{\phi}$ and w_F such that

$$\boldsymbol{z} = [\boldsymbol{w} \ \ \boldsymbol{\phi} \ \ w_F]^{\ T}.$$

The matrices $\mathcal{M}$, $\mathcal{K}$ and $\mathcal{D}$ are all partitioned in the same way and we describe the partitioning for $\mathcal{M}$:

$$\mathcal{M} = \begin{bmatrix} \mathcal{M}_{11} & \mathcal{M}_{12} & \mathcal{M}_{13} \\ \mathcal{M}_{21} & \mathcal{M}_{22} & \mathcal{M}_{23} \\ \mathcal{M}_{31} & \mathcal{M}_{32} & \mathcal{M}_{33} \end{bmatrix},$$

where $\mathcal{M}_{11}$, $\mathcal{M}_{12}$, $\mathcal{M}_{21}$, and $\mathcal{M}_{22}$ are all $(2n+2) \times (2n+2)$ matrices.

$\mathcal{M}_{31}$, $\mathcal{M}_{32}$, $(\mathcal{M}_{13})^T$ and $(\mathcal{M}_{23})^T$ are all $1 \times (2n+2)$ matrices and $\mathcal{M}_{33}$ is a 1×1 matrix.

Denoting the entries for the partitioned matrices with superscripts in brackets, we find the following results.

$$\mathcal{M}_{11}^{(11)} = M_{11} + m_F \quad \text{and} \quad \mathcal{M}_{11}^{(ij)} = M_{ij} \quad \text{otherwise},$$

$$\mathcal{M}_{22} = \frac{1}{\alpha} M \quad \text{and} \quad \mathcal{M}_{33} = I_F.$$

All the other partitioned matrices in $\mathcal{M}$ are zero matrices.

$$\mathcal{K}_{11}^{(11)} = K_{11} + K_F \quad \text{and} \quad \mathcal{K}_{11}^{(ij)} = K_{ij} \quad \text{otherwise},$$

$$\mathcal{K}_{12} = -L \quad \text{and} \quad \mathcal{K}_{21} = -(L^T + \mu P),$$

$$\mathcal{K}_{22}^{(11)} = \frac{1}{\beta} K_{11} + M_{11} + k \quad \text{and} \quad \mathcal{K}_{22}^{(ij)} = \frac{1}{\beta} K_{ij} + M_{ij} \quad \text{otherwise},$$

$$\mathcal{K}_{32}^{(11)} = -k \quad \text{and} \quad \mathcal{K}_{32}^{(1j)} = 0 \quad \text{otherwise},$$

$$\mathcal{K}_{23} = \mathcal{K}_{32}^T \quad \text{and} \quad \mathcal{K}_{33} = k + k_F.$$

All the other partitioned matrices in $\mathcal{K}$ are zero matrices.

$$\mathcal{D}_{11}^{(11)} = C_F \quad \text{and} \quad \mathcal{D}_{11}^{(ij)} = 0 \quad \text{otherwise},$$

University of Pretoria etd – Labuschagne, A (2006)

$$\mathcal{D}_{22}^{(11)} = c \quad \text{and} \quad \mathcal{D}_{22}^{(ij)} = 0 \quad \text{otherwise,}$$

$$\mathcal{D}_{32}^{(11)} = -c \quad \text{and} \quad \mathcal{D}_{32}^{(1j)} = 0 \quad \text{otherwise,}$$

$$\mathcal{D}_{23} = (\mathcal{D}_{32})^T \quad \text{and} \quad \mathcal{D}_{33}^{(11)} = c + c_F\,.$$

All the other partitioned matrices in $\mathcal{D}$ are zero matrices.

Problem VTE 4

We define $\boldsymbol{w}$ and $\boldsymbol{\phi}$ as the $4n+7$ column vector $\boldsymbol{z}$

$$\boldsymbol{z} = [\boldsymbol{w} \;\; \boldsymbol{\phi} \;\; \theta_B \;\; w_F \;\; \theta_F]^{\,T}.$$

The matrices $\mathcal{M}$, $\mathcal{K}$ and $\mathcal{D}$ are partitioned in the same way and a description for the matrix $\mathcal{M}$ follows.

$$\mathcal{M} = \begin{bmatrix} \mathcal{M}_{11} & \mathcal{M}_{12} & \mathcal{M}_{13} \\ \mathcal{M}_{21} & \mathcal{M}_{22} & \mathcal{M}_{23} \\ \mathcal{M}_{31} & \mathcal{M}_{32} & \mathcal{M}_{33} \end{bmatrix},$$

where $\mathcal{M}_{11}$, $\mathcal{M}_{12}$, $\mathcal{M}_{21}$, and $\mathcal{M}_{22}$ are all $(2n+2)\times(2n+2)$ matrices.

$\mathcal{M}_{31}$, $\mathcal{M}_{32}$, $(\mathcal{M}_{13})^T$ and $(\mathcal{M}_{23})^T$ are all $3\times(2n+2)$ matrices and $\mathcal{M}_{33}$ is a 3×3 matrix.

We have that

$$\mathcal{M}_{11}^{(11)} = M_{11} + m_B \quad \text{and} \quad \mathcal{M}_{11}^{(ij)} = M_{ij} \quad \text{otherwise,}$$

$$\mathcal{M}_{22} = \frac{1}{\alpha}\, M \quad \text{and} \quad \mathcal{M}_{33} = \begin{bmatrix} I_B & 0 & 0 \\ 0 & m_F & 0 \\ 0 & 0 & I_F \end{bmatrix}.$$

All the other partitioned matrices in $\mathcal{M}$ are zero matrices.

$$\mathcal{K}_{11}^{(11)} = K_{11} + K_{FB} \quad \text{and} \quad \mathcal{K}_{11}^{(ij)} = K_{ij} \quad \text{otherwise,}$$

$$\mathcal{K}_{12} = -L \quad \text{and} \quad \mathcal{K}_{21} = -(L^T + \mu P)\,,$$

$$\mathcal{K}_{22}^{(11)} = \frac{1}{\beta}\, K_{11} + M_{11} + k_{BA} \quad \text{and} \quad \mathcal{K}_{22}^{(ij)} = \frac{1}{\beta}\, K_{ij} + M_{ij} \quad \text{otherwise,}$$

$$\mathcal{K}_{31}^{(21)} = -K_{FB} \quad \text{and} \quad \mathcal{K}_{31}^{(ij)} = 0 \quad \text{otherwise,}$$

University of Pretoria etd – Labuschagne, A (2006)

$$\mathcal{K}_{32}^{(11)} = -k_{BA} \quad \text{and} \quad \mathcal{K}_{32}^{(ij)} = 0 \quad \text{otherwise},$$

$$\mathcal{K}_{13} = \mathcal{K}_{31}^T \quad \text{and} \quad \mathcal{K}_{23} = \mathcal{K}_{32}^T.$$

$$\mathcal{K}_{33} = \begin{bmatrix} (k_{BA} + k_{FB}) & 0 & -k_{FB} \\ 0 & (K_{FB} + K_F) & 0 \\ -k_{FB} & 0 & (k_{FB} + k_F) \end{bmatrix}.$$

All the other partitioned matrices in $\mathcal{K}$ are zero matrices.

$$\mathcal{D}_{11}^{(11)} = C_{FB} \quad \text{and} \quad \mathcal{D}_{11}^{(ij)} = 0 \quad \text{otherwise},$$

$$\mathcal{D}_{22}^{(11)} = c_{BA} \quad \text{and} \quad \mathcal{D}_{22}^{(ij)} = 0 \quad \text{otherwise},$$

$$\mathcal{D}_{31}^{(21)} = -C_{FB} \quad \text{and} \quad \mathcal{D}_{31}^{(ij)} = 0 \quad \text{otherwise},$$

$$\mathcal{D}_{32}^{(11)} = -c_{BA} \quad \text{and} \quad \mathcal{D}_{32}^{(ij)} = 0 \quad \text{otherwise},$$

$$\mathcal{D}_{13} = \mathcal{D}_{31}^T \quad \text{and} \quad \mathcal{D}_{23} = \mathcal{D}_{32}^T,$$

$$\mathcal{D}_{33} = \begin{bmatrix} (c_{BA} + c_{FB}) & 0 & -c_{FB} \\ 0 & (C_{FB} + C_F) & 0 \\ -c_{FB} & 0 & (c_{FB} + c_F) \end{bmatrix}.$$

6.5 Numerical results

In [LVV], the Rayleigh and Euler-Bernoulli models were used to find the first four frequencies for the Newland chimney. The first two models were discussed in detail in [LVV] and will not be discussed here. The contribution due to gravity was approximated in [LVV], whereas we use the exact value for the integral $\int_0^1 (1-x)\partial_x w(x,t)dx$ in the finite element approximation. The effect of the approximation of the above mentioned integral to the exact value is minimal. We found that results differ with less than 1%.

Approximations for the eigenvalue problems VRE 3, VRE 4, VTE 3 and VTE 4 are found with the finite element method. MATLAB codes were written for calculating the $\mathcal{M}$, $\mathcal{D}$ and $\mathcal{K}$ matrices for these problems and the standard MATLAB routines were used for solving the quadratic eigenvalue problems.

University of Pretoria etd – Labuschagne, A (2006)

6.5.1 Physical constants

For the purpose of comparing our results with those of Newland, the values for the physical constants that we use are displayed in Table 1.

The results are found for a typical steel chimney of height $\ell = 42\,m$, mass $21\,000\,kg$, diameter $D = 2.25\,m$ and wall thickness $t = 6.8\,mm$. Young's modulus E is taken as $E = 2.1 \times 10^{11}$ and $\rho A = 500$. Approximations for I and A are used, with $I \approx \dfrac{\pi D^3 t}{8}$ and $A \approx \pi D t$. We choose $\dfrac{G}{E} = \dfrac{3}{8}$ and $\kappa^2 = \dfrac{2}{3}$.

Table 1: Constants

	Model 3		Model 4	
	(Physical)	(Dimensionless)	(Physical)	(Dimensionless)
m_B			500	2.3810×10^{-2}
m_F	3×10^5	1.4286×10^1	3×10^5	1.4286×10^1
I_B			300	8.0985×10^{-6}
I_F	1.5×10^6	4.0492×10^{-2}	1.5×10^6	4.0492×10^{-2}
K_{FB}			1×10^{10}	1.6644×10^2
K_F	2×10^{10}	3.3287×10^2	2×10^{10}	3.3287×10^2
C_{FB}			1×10^7	8.9026×10^0
C_F	1×10^7	8.9026×10^0	1×10^7	8.9026×10^0
k_{FB}			1×10^{10}	9.4352×10^{-2}
k_F	6×10^{10}	5.6611×10^{-1}	6×10^{10}	5.6611×10^{-1}
c_{FB}			2×10^7	1.0094×10^{-2}
c_F	2×10^7	1.0094×10^{-2}	2×10^7	1.0094×10^{-2}
k_{BA}			2×10^9	1.8870×10^{-2}
c_{BA}			1×10^6	5.0468×10^{-4}

We find that $\mu = 8.1637 \times 10^{-5}$ and $\beta = 6.9689 \times 10^2$.

For Problems VRE 3 and VRE 4, the constants must satisfy the inequalities

$$1 > 2\mu\beta, \quad k_{BA} > 4\mu, \quad k_{FB} > 8\mu \quad \text{and} \quad k_F > 8\mu$$

in order to assure a unique solution (see Section 3.2). It is clear that these conditions are met with our choice of constants.

University of Pretoria etd – Labuschagne, A (2006)

6.5.2 Convergence

The convergence of the first four eigenvalues is established empirically by increasing the number of elements. Note that the eigenvalues are complex. We consider the imaginary part of the eigenvalues. Convergence on the real parts of the eigenvalues is also established, but not displayed.

Experiments on the convergence of the eigenvalues were done for the cases $\mu = 0$ and $\mu \neq 0$. Results for for the case that $\mu = 0$ for Problems VRE 4 and VTE 4 are given in Tables 2 and 3 respectively. The other cases yield similar results. The eigenvalues occur in complex conjugate pairs and we only list the imaginary parts. From the tables we see that the displayed eigenvalues are accurate to 5 significant digits.

Table 2: Imaginary parts of the eigenvalues Problem VRE 4 ($\mu = 0$)

j	$Im(\lambda_1^{(j)})$	$Im(\lambda_2^{(j)})$	$Im(\lambda_3^{(j)})$	$Im(\lambda_4^{(j)})$
10	6.063598992319	39.20328150732	111.2984099726	200.5292536731
20	6.063595477419	39.20234445416	111.2772664612	200.5237167363
40	6.063595255872	39.20228511054	111.2759080178	200.5233527121
80	6.063595480677	39.20228147057	111.2758225750	200.5233296975
160	6.063597520788	39.20228156442	111.2758174750	200.5233097736

Table 3: Imaginary parts of the eigenvalues Problem VTE 4 ($\mu = 0$)

j	$Im(\lambda_1^{(j)})$	$Im(\lambda_2^{(j)})$	$Im(\lambda_3^{(j)})$	$Im(\lambda_4^{(j)})$
10	6.048681000262	38.57139344125	107.1242256458	199.6387452859
20	6.048680557234	38.57127388156	107.1215429222	199.6359153764
40	6.048680548363	38.57127156531	107.1214873202	199.6358505940
80	6.048680543847	38.57127152495	107.1214863566	199.6358494317
160	6.048680553394	38.57127152813	107.1214863407	199.6358494379

6.5.3 Effect of gravity, rotary inertia and shear

Recall that the inclusion of gravity in Problems VRE 3 and VRE 4 yield symmetrical bilinear forms, which is desirable from a theoretical point of

University of Pretoria etd – Labuschagne, A (2006)

view (see Section 3.2.) However, gravity is excluded in the formulation of Problems VTE 3 and VTE 4, since inclusion results in a non-symmetric bilinear form b. The existence and uniqueness of the solution in this case has not been proved (see Section 3.3). Adapting Problems VTE 3 and VTE 4 to include gravity, "solutions" for the Timoshenko models with gravity are simulated. This is done to compare results to Problems VRE 3 and VRE 4 with the gravity term included and omitted. A comparison on the imaginary part of the eigenvalues for all these cases are displayed in Table 4. We list only the positive values for the imaginary part (since the eigenvalues occur in complex conjugate pairs).

Table 4: Effect of gravity

	Euler-Bernoulli		Rayleigh		Timoshenko	
	$\mu = 0$	$\mu \neq 0$	$\mu = 0$	$\mu \neq 0$	$\mu = 0$	$\mu \neq 0$
$Im(\lambda_1)$	6.0680	6.0584	6.0636	6.0540	6.0487	6.0418
$Im(\lambda_2)$	39.408	39.407	39.202	39.201	38.571	38.592
$Im(\lambda_3)$	112.70	112.70	111.28	111.28	107.12	107.14
$Im(\lambda_4)$	200.72	200.72	200.52	200.52	199.64	199.64

Denoting the eigenvalues by λ_k^{EB}, λ_k^R and λ_k^T for $k = 1$, 2, 3 and 4, we observe that

$$Im(\lambda_k^{EB}) > Im(\lambda_{kc}^R) > Im(\lambda_{kc}^T)\,,$$

which is to be expected.

The effect of rotary inertia is negligible (Rayleigh model versus Euler-Bernoulli model). The maximum relative error for comparable eigenvalues is less than 1%. The effect of shear, although slightly larger than the effect of rotary inertia, is also negligible (Timoshenko model versus Euler-Bernoulli model).

Comparing results for the three models with respect to the gravity term, shows that the influence of gravity is minimal. The maximum relative error (with respect to the case $\mu = 0$) for all three models is less than 0.2% and this occurs for the first eigenvalue.

6.5.4 Conclusion

From the results we see that the effect of rotary inertia, shear and gravity is minimal.

University of Pretoria etd – Labuschagne, A (2006)

We conclude that using more complex models for calculating eigenvalues is not justified. Implementation of the finite element method is more complex for the models that include the above mentioned factors. It is therefore sufficient to use the Euler-Bernoulli model for finding the first four eigenvalues.

University of Pretoria etd – Labuschagne, A (2006)

Chapter 7

Cantilever beam

7.1 Scope of the investigation

As indicated in Section 1.5, we are concerned with the Euler-Bernoulli and Timoshenko models for a cantilever beam. In this section we provide more detail.

Eigenvalues

We start with a comparison of eigenvalues for the two models. Depending on the parameter α, a number of small eigenvalues do not differ significantly. For a beam with square cross sectional area $h \times h$,

$$\alpha = 12 \left(\frac{\ell}{h} \right)^2$$

and a value of $\alpha = 1200$ represents a beam of length to height ratio $10 : 1$, whereas $\alpha = 300$ is associated with a beam of length to height ratio $5 : 1$.

The first four eigenvalues for $\alpha = 4800$, $\alpha = 1200$ and $\alpha = 300$ are presented in Table 1.

University of Pretoria etd – Labuschagne, A (2006)

Table 1: Comparison of eigenvalues

$\alpha = 4800$

	Euler-Bernoulli	Timoshenko
λ_1	1.030×10^{-2}	1.025×10^{-2}
λ_2	4.046×10^{-1}	3.914×10^{-1}
λ_3	3.172×10^{0}	2.937×10^{0}
λ_4	1.218×10^{1}	1.062×10^{1}

$\alpha = 1200$

	Euler-Bernoulli	Timoshenko
λ_1	3.214×10^{-2}	3.164×10^{-2}
λ_2	1.262×10^{0}	1.136×10^{0}
λ_3	9.897×10^{0}	7.862×10^{0}
λ_4	3.800×10^{1}	2.587×10^{1}

$\alpha = 300$

	Euler-Bernoulli	Timoshenko
λ_1	1.286×10^{-1}	1.209×10^{-1}
λ_2	5.049×10^{0}	3.507×10^{0}
λ_3	3.959×10^{1}	1.987×10^{1}
λ_4	1.520×10^{2}	5.477×10^{1}

The first three eigenvalues differ slightly for the case $\alpha = 4800$. It is doubtful if this is of practical importance. If $\alpha = 1200$, the first eigenvalues are close. For $\alpha = 300$, the first eigenvalue differs significantly and the others differ dramatically. However, one may question the applicability of beam theory in this case.

The two-dimensional model for a cantilever beam should be closer to reality than a one-dimensional model. In Section 7.7 we compute the eigenvalues and corresponding eigenfunctions for the two-dimensional beam and compare the results to those of the Timoshenko and Euler-Bernoulli models. We also consider the case $\alpha = 300$ to determine whether beam theory is still applicable.

Alternative boundary condition

Consider the alternative boundary conditions in Section 2.2. Results for this model will differ little from those obtained with the conventional boundary conditions if $c_{ij} \approx 0$, i.e. d_{ij} large. (Recall that $D = C^{-1}$.)

University of Pretoria etd – Labuschagne, A (2006)

The weak variational form for the cantilever Timoshenko beam is presented in Section 3.1. The bilinear form b for the alternative boundary condition is presented in Section 3.4. If λ_1 is the smallest eigenvalue, then

$$\lambda_1 = R(v) = \min\left\{b(v,v) \;\middle|\; \|v\|_X = 1\right\}$$

where R is the Rayleigh quotient. Since

$$b(v,v) \;=\; \frac{1}{\beta}\|v_2'\|^2 + \|v_1' - v_2\|^2 + [\gamma v_1 \;\gamma v_2]\; D\; [\gamma v_1 \;\gamma v_2]^T\,,$$

the eigenvalue λ_1 increases as the elements d_{ij} of D increase. This implies that the first eigenvalue is always less than the first eigenvalue for the conventional boundary conditions. This is why the alternative model will amplify the difference between the two models. It serves no purpose to investigate the alternative boundary condition any further and more can be achieved by consideration of two-dimensional or three-dimensional models.

Equilibrium problem

Since the shear stress is a multiple of the shear strain and we are interested in qualitative results, it is irrelevant whether we consider the stress distribution or the strain distribution. Our main concern is the shear at the built in end. We use solutions of the equilibrium problem, Problem CTD 1, to determine the shear strain in the two-dimensional cantilever beam.

The solution of Problem CTD 1 also yields the deflection and we compare the results to the deflection for the Euler-Bernoulli and Timoshenko models.

7.2 Boundary conditions and test functions

7.2.1 Boundary conditions

The boundary conditions given in Section 2.3 were of a general nature. In this section we provide more detail. In an effort to model the built in end of a beam, we consider three configurations, which are described below. The first configuration is commonly used but it can not be used to investigate shear at the cross section where we have the transition from clamped to free.

University of Pretoria etd – Labuschagne, A (2006)

Note that for all three configurations the boundary consists of parts Σ and Γ, and that the boundary Σ is made up by the parts as shown below in the description for the different configurations. For the equilibrium problem and the eigenvalue problem, the conditions on Σ remain the same for both Problems CTD 1 and CTD 2, and are listed in the tables. However, the conditions on Γ differ for the two problems: For Problem CTD 1 the traction $\boldsymbol{t} = t\boldsymbol{e}_2$ with t a positive function and Γ is stress free for Problem CTD 2.

Configuration 1: Fixed beam

For this problem we assume that the beam is fixed rigidly to the support at $x_1 = 0$. The reference configuration is the rectangle $0 \leq x_1 \leq \ell$ and $0 \leq x_2 \leq h$. In this case the displacements are zero on Σ_0 and the two parts of Σ_1 are stress free.

Reference Configuration 1

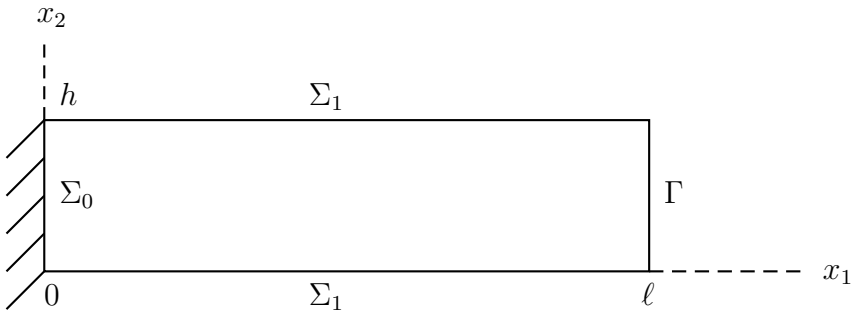

Boundary conditions for Configuration 1

Section	Coordinates	Conditions
Σ_0	$x_1 = 0, \quad 0 < x_2 < h$	$u_1 = u_2 = 0$
Σ_1	$0 < x_1 < \ell, \quad x_2 = 0$	$T\boldsymbol{e}_2 = \boldsymbol{0}$
	$0 < x_1 < \ell, \quad x_2 = h$	$T\boldsymbol{e}_2 = \boldsymbol{0}$
Γ	$x_1 = \ell, \quad 0 < x_2 < h$	$T\boldsymbol{e}_1 = t\boldsymbol{e}_2$ (Equilibrium problem) $T\boldsymbol{e}_1 = \boldsymbol{0}$ (Eigenvalue problem)

University of Pretoria etd – Labuschagne, A (2006)

Configuration 2: Built in beam - case I

In this case we assume that a section of the beam is embedded in an inelastic support as in the diagram below. The reference configuration is the rectangle $-a \leq x_1 \leq \ell$ and $0 \leq x_2 \leq h$. The boundary Σ_1 is stress free.

Reference Configuration 2

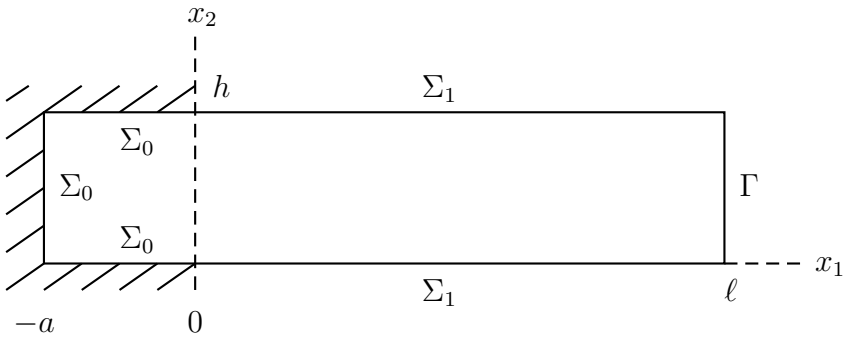

Boundary conditions for Configuration 2

Section	Coordinates	Conditions
Σ_0	$-a < x_1 < 0, \quad x_2 = 0$	$u_1 = u_2 = 0$
	$-a < x_1 < 0, \quad x_2 = h$	$u_1 = u_2 = 0$
	$x_1 = -a, \quad 0 < x_2 < h$	$u_1 = u_2 = 0$
Σ_1	$0 < x_1 < \ell, \quad x_2 = 0$	$T\boldsymbol{e}_2 = \boldsymbol{0}$
	$0 < x_1 < \ell, \quad x_2 = h$	$T\boldsymbol{e}_2 = \boldsymbol{0}$
Γ	$x_1 = \ell, \quad 0 < x_2 < h$	$T\boldsymbol{e}_1 = t\boldsymbol{e}_2$ (Equilibrium problem) $T\boldsymbol{e}_1 = \boldsymbol{0}$ (Eigenvalue problem)

Configuration 3: Built in beam - case II

In this case we still assume that a section of the beam is embedded in an inelastic support. The forced boundary conditions in Configuration 2 are mathematically convenient but not completely realistic, since "negative pressures" on the beam are possible. To avoid this, we consider Configuration 3

University of Pretoria etd – Labuschagne, A (2006)

for Problem CTD 1. The reference configuration is the rectangle $-a \leq x_1 \leq \ell$ and $0 \leq x_2 \leq h$, x_2 being vertical. The results from Configuration 2 were used to specify the boundary conditions for Configuration 3 to make them more realistic.

Reference Configuration 3

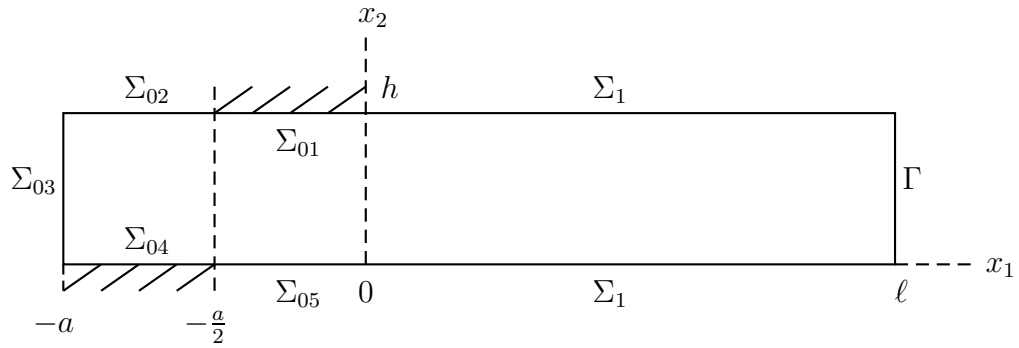

Boundary conditions for Configuration 3

Section	Coordinates	Conditions
Σ_{01}	$-\frac{a}{2} < x_1 < 0, \quad x_2 = h$	$u_2 = 0 \;\; \& \;\; \sigma_{12} = 0$
Σ_{02}	$-a < x_1 < -\frac{a}{2}, \quad x_2 = h$	$T\boldsymbol{e}_2 = \boldsymbol{0}$
Σ_{03}	$x_1 = -a, \quad 0 < x_2 < h$	$u_1 = 0 \;\; \& \;\; \sigma_{12} = 0$
Σ_{04}	$-a < x_1 < -\frac{a}{2}, \quad x_2 = 0$	$u_2 = 0 \;\; \& \;\; \sigma_{12} = 0$
Σ_{05}	$-\frac{a}{2} < x_1 < 0, \quad x_2 = 0$	$T\boldsymbol{e}_2 = \boldsymbol{0}$
Σ_1	$0 < x_1 < \ell, \quad x_2 = 0$	$T\boldsymbol{e}_2 = \boldsymbol{0}$
	$0 < x_1 < \ell, \quad x_2 = h$	$T\boldsymbol{e}_2 = \boldsymbol{0}$
Γ	$x_1 = \ell, \quad 0 < x_2 < h$	$T\boldsymbol{e}_1 = \boldsymbol{0}$

7.2.2 Test functions

The test functions must satisfy the forced boundary conditions as specified in Section 2.3. A vector valued function $\boldsymbol{\phi}$ is a test function if each component $\phi_i \in C^1(\bar{\Omega})$ and $\phi_i = 0$ on some part of Σ.

For the three Configurations the set of test functions are as follows.

University of Pretoria etd – Labuschagne, A (2006)

Configuration 1

$$T(\Omega) = \left\{ \boldsymbol{\phi} \in C^1(\bar{\Omega})^2 \;\middle|\; \boldsymbol{\phi} = \mathbf{0} \text{ on } \Sigma_0 \right\}$$

Configuration 2

$$T(\Omega) = \left\{ \boldsymbol{\phi} \in C^1(\bar{\Omega})^2 \;\middle|\; \boldsymbol{\phi} = \mathbf{0} \text{ on } \Sigma_0 \right\}$$

Configuration 3

$$T(\Omega) = \left\{ \boldsymbol{\phi} \in C^1(\bar{\Omega})^2 \;\middle|\; \phi_1 = 0 \text{ on } \Sigma_{03} \text{ and } \phi_2 = 0 \text{ on } \Sigma_{01} \text{ and } \Sigma_{04} \right\}$$

7.3 Galerkin approximation

We consider Problems CTD 1 and CTD 2 with the three configurations as discussed in Section 7.2.1 but in a finite dimensional subspace of $T(\Omega)$.

Consider a set of basis functions

$$\{\delta_1,\, \delta_2,\, \ldots\, \delta_p\}$$

and set

$$\boldsymbol{u}^h \;=\; \begin{bmatrix} u_1^h & u_2^h \end{bmatrix}^T \;=\; \left[\sum_{j=1}^{p} \delta_j u_{1j} \quad \sum_{j=1}^{p} \delta_j u_{2j} \right]^T .$$

The set with elements

$$[\delta_1\; 0]^T, \quad [\delta_2\; 0]^T, \quad \ldots \quad [\delta_p\; 0]^T,$$

$$[0,\; \delta_1]^T, \quad [0,\; \delta_2]^T, \quad \ldots \quad [0,\; \delta_p]^T$$

now is a basis for

$$S^h = \left\{ \left[\sum_{j=1}^{p} \delta_j u_{1j} \quad \sum_{j=1}^{p} \delta_j u_{2j} \right]^T \;\middle|\; u_{1j} \;\text{ and }\; u_{2j} \;\in I\!R \right\}$$

University of Pretoria etd – Labuschagne, A (2006)

7.3.1 Equilibrium problem

For the equilibrium problem we consider the case that a (dimensionless) vertical force F is applied at $x_1 = 1$. This leads to

$$\boldsymbol{t} = \begin{bmatrix} \sigma_{11} \\ \sigma_{21} \end{bmatrix} = \begin{bmatrix} 0 \\ t \end{bmatrix} . \tag{7.3.1}$$

Note that t is a function of x_2 and $F = \int_0^h t(x_2)\, dx_2$. An obvious possibility is to choose t constant, but it is important to realize that such a choice is arbitrary and that it is advisable to consider other possibilities.

Galerkin approximation

The Galerkin approximation for the equilibrium problem is formulated.

Find $\boldsymbol{u}^h \in S^h$ so that

$$b(\boldsymbol{u}^h, \boldsymbol{\phi}) = \int_\Gamma \boldsymbol{t} \cdot \boldsymbol{\phi}\, ds \quad \forall \quad \boldsymbol{\phi} \in \ S^h.$$

To find the Galerkin approximation for the problem in variational form, we substitute $\boldsymbol{\phi} = [\phi_1,\ \phi_2]^T$ with

$$[\,\delta_1\,,\ 0\,]^T\,,\ [\,\delta_2\,,\ 0\,]^T\,,\ \ldots\ [\,\delta_p\,,\ 0\,]^T\,,$$

and

$$[\,0,\ \delta_1\,]^T\,,\ [\,0,\ \delta_2\,]^T\,,\ \ldots\ [0,\ \delta_p\,]^T\,.$$

in the variational form.

For the remainder of this chapter, we use the notation

$$(f, g) = \iint_\Omega f g\,,$$

where Ω denotes the reference configuration.

University of Pretoria etd – Labuschagne, A (2006)

We obtain the following system of linear equations:

$$\frac{\big(\partial_1 u_1^h + \nu\partial_2 u_2^h,\ \partial_1\delta_i\big)}{\gamma(1-\nu^2)} + \frac{\big(\partial_1 u_2^h + \partial_2 u_1^h,\ \partial_2\delta_i\big)}{2\gamma(1+\nu)} = 0 \quad \text{for } i = 1,\ 2,\ \ldots,\ p \tag{7.3.2}$$

$$\frac{\big(\partial_2 u_2^h + \nu\partial_1 u_1^h,\ \partial_2\delta_i\big)}{\gamma(1-\nu^2)} + \frac{\big(\partial_1 u_2^h + \partial_2 u_1^h,\ \partial_1\delta_i\big)}{2\gamma(1+\nu)} = \int_0^h t(x_2)\delta_i(1,x_2)dx_2, \quad \text{for } i = 1,\ 2,\ \ldots,\ p \tag{7.3.3}$$

7.3.2 The eigenvalue problem

Galerkin approximation

Find $\boldsymbol{u}^h \in S^h$ so that

$$b(\boldsymbol{u}^h, \boldsymbol{\phi}) = \lambda \iint_\Omega \boldsymbol{u}^h \cdot \boldsymbol{\phi}\, dA \quad \forall \ \boldsymbol{\phi} \in \ S^h\,.$$

Following the same procedure as in Section 7.3.1, we find the Galerkin approximation by solving the following system of linear equations:

$$\frac{\big(\partial_1 u_1^h + \nu\partial_2 u_2^h,\ \partial_1\delta_i\big)}{\gamma(1-\nu^2)} + \frac{\big(\partial_1 u_2^h + \partial_2 u_1^h,\ \partial_2\delta_i\big)}{2\gamma(1+\nu)} = \lambda\big(u_1, \delta_i\big) \quad \text{for } i = 1,\ 2,\ \ldots,\ p \tag{7.3.4}$$

$$\frac{\big(\partial_2 u_2^h + \nu\partial_1 u_1^h,\ \partial_2\delta_i\big)}{\gamma(1-\nu^2)} + \frac{\big(\partial_1 u_2^h + \partial_2 u_1^h,\ \partial_1\delta_i\big)}{2\gamma(1+\nu)} = \lambda\big(u_2, \delta_i\big) \quad \text{for } i = 1,\ 2,\ \ldots,\ p \tag{7.3.5}$$

7.4 Matrix formulation

We use the bicubic basis functions described in Section 4.2. We divide Ω in rs rectangular elements, where r denotes the number of intervals on the

University of Pretoria etd – Labuschagne, A (2006)

x_1-axis and s the number of elements on the x_2-axis. The number of nodes for this grid is $N = (r+1)(s+1)$ and hence the number of bicubic basis functions is $4N$. Hence $p = 4N$ in the description in Sections 7.3.1 and 7.3.2.

The approximate solution is denoted by $\boldsymbol{u}^h$ and the components u_1 and u_2 are expressed as a linear combination of bicubic basis functions δ_j as

$$u_i^h(x) = \sum_{j=1}^{4N} \delta_j(x)\, u_{ij}\,.$$

For the equilibrium problem we define a load vector $\boldsymbol{c}$ with the two components $\boldsymbol{c}_1$ and $\boldsymbol{c}_2$. In this case $\boldsymbol{c}_1 = \boldsymbol{0}$ and the i-th component of $\boldsymbol{c}_2$ is

$$c_{2i} = \int_0^h t(x_2)\delta_i(1, x_2)dx_2\,.$$

The Galerkin approximations for both Problems CTD 1 and CTD 2 for the different configurations can now be be written in matrix form. The different configurations determine which of the coefficients u_{1j} and u_{2j} for $j = 1,\, 2,\, \ldots\, 4N$ are zero.

For the equilibrium problem the matrix form is given by

$$\mathcal{K}\boldsymbol{u} = \boldsymbol{c},$$

and for the eigenvalue problem the matrix form is

$$\mathcal{K}\boldsymbol{u} = \lambda\mathcal{M}\boldsymbol{u}.$$

The matrices $\mathcal{K}$ and $\mathcal{M}$ will differ for the different configurations.

7.4.1 Construction of the matrices $\mathcal{K}$ and $\mathcal{M}$

To construct $\mathcal{K}$ and $\mathcal{M}$, the following matrices are needed:

$$K_{pq} = \Big((\partial_p\delta_j,\ \partial_q\delta_i) \Big)_{4N\times 4N} \qquad \text{where} \quad p = 1,\ 2 \quad \text{and} \quad q = 1,\ 2$$

$$\text{and} \quad M = \Big((\delta_j,\ \delta_i) \Big)_{4N\times 4N}$$

Note that $K_{12} = K_{21}$.

University of Pretoria etd – Labuschagne, A (2006)

Define the following matrices:

$$K_{11}^{\Omega} = K_{11} + \frac{(1-\nu)}{2} K_{22}, \qquad K_{12}^{\Omega} = \nu K_{21} + \frac{(1-\nu)}{2} K_{12}$$

$$K_{21}^{\Omega} = \nu K_{12} + \frac{(1-\nu)}{2} K_{21}, \qquad K_{22}^{\Omega} = K_{22} + \frac{(1-\nu)}{2} K_{11}$$

$$M_{11}^{\Omega} = M, \qquad M_{12}^{\Omega} = O, \qquad M_{21}^{\Omega} = O, \qquad M_{22}^{\Omega} = M$$

Define the $8N \times 8N$ matrices

$$K^{\Omega} = \begin{bmatrix} K_{11}^{\Omega} & K_{12}^{\Omega} \\ K_{21}^{\Omega} & K_{22}^{\Omega} \end{bmatrix} \quad \text{and} \quad M^{\Omega} = \begin{bmatrix} M_{11}^{\Omega} & M_{12}^{\Omega} \\ M_{21}^{\Omega} & M_{22}^{\Omega} \end{bmatrix}.$$

Let $\boldsymbol{u}_i = [\, u_{i1} \;\; u_{i2} \;\; \cdots \;\; u_{i,4N} \,]^T$ for $i = 1$ and $i = 2$ and $\boldsymbol{u}^{\Omega} = [\, \boldsymbol{u}_1 \;\; \boldsymbol{u}_2 \,]^T$.

Define $\boldsymbol{c}^{\Omega} = [\, \mathbf{0} \;\; \boldsymbol{b} \,]^T$ with $\mathbf{0}$ a $4N \times 1$ zero matrix.

The vector $\boldsymbol{b}$ is a $4N \times 1$ matrix that results from the line integral $\int_{\Gamma} \boldsymbol{t} \cdot \boldsymbol{\phi}\, ds$.

The matrices $\mathcal{K}$, $\mathcal{M}$, $\boldsymbol{u}$ and $\boldsymbol{c}$ are found from K^{Ω}, M^{Ω}, $\boldsymbol{u}^{\Omega}$ and $\boldsymbol{c}^{\Omega}$ respectively by omitting appropriate rows and columns, according to the restrictions on the test functions.

The test functions must satisfy the forced boundary conditions, and when we use the bicubic basis functions, care must be taken that the "not so obvious" basis functions are also omitted. As an example, consider Configuration 1 for which $u_1 = u_2 = 0$ on Σ_0. Then the tangential derivatives $\partial_2 u_1 = \partial_2 u_2 = 0$ on Σ_0.

Remark

For the mixed derivatives equal to zero in Configuration 3, recall that $\sigma_{21} = 0$ and therefore $\partial_1 u_2 + \partial_2 u_1 = 0$.

7.5 Shear strain distribution

In this section we determine the shear strain profiles for a built in beam. For the reason given earlier, we consider Problem CTD 1 with Configuration 3.

University of Pretoria etd – Labuschagne, A (2006)

To be more specific, we determine the shear strain distribution in the region where there is a transition from contact to free surface.

A beam of length 1.1, width 0.1 and height $h = 0.1$ is considered. The built in part of the beam has length $a = 0.1$. For experimental results, we used the constants (see Section 1.2.4)

$$\nu = 0.3 \quad \text{and} \quad \kappa^2 = \frac{5}{6}\,.$$

In the initial numerical experiments, we computed the shear strain for the entire beam with a constant stress t on the right hand side of the beam, namely $t(x_2) = 0.001$. Experiments show that to obtain accurate results, refining the grid in the x_2-direction is essential.

The stress distribution in the middle of the beam (for x_1-values roughly between 0.15 and 0.85), follows a "parabolic profile" which varies little. This is in line with the theory ([Fu, Sec 7.7] and [My, Sec 9.2]). From these results we find, with the given physical constants, an approximation for the stress distribution

$$\sigma_{21}(x_1, x_2) \approx -6x_2^2 + 0.6x_2.$$

To obtain accurate results, the stress profile in the middle of the beam is used as an input on a part of the original beam. We consider the part of the beam of length 0.25. The first part of length 0.1 coincides with the built in end of the original beam and the part of length 0.15 with the free part closest to the built in end.

The results are interpreted graphically in Figure 1, where the stress profiles are plotted at specified x_1-values. In each graph, the vertical axis denotes the x_2-axis, whereas the horizontal axis is the σ_{21}-axis for the specified x_1-value that is shown at the bottom of each graph. The scale on the axes stay throughout the same for all the graphs, in order to compare stress profiles at different x_1-values. Each interval shown on the horizontal axis has a length of 0.002 and the length of the interval shown on the vertical axis is 0.1.

For the profiles at $x_1 = 0.1$ and $x_1 = 0.2$, the values for σ_{21} have magnitudes that are quite large in magnitude close to $x_2 = 0.1$. This explains the arrowheads in these two graphs. It is clear that the shear stress distribution exhibits enormous variation in a small interval containing $x_1 = 0$. We conclude that the constitutive equation (1.2.8) is not valid in this interval. (Recall the remarks in Section 1.2.2.) However, the phenomenon observed is not sufficient to reject the Timoshenko model.

University of Pretoria etd – Labuschagne, A (2006)

Figure 1: Stress profiles at built in end

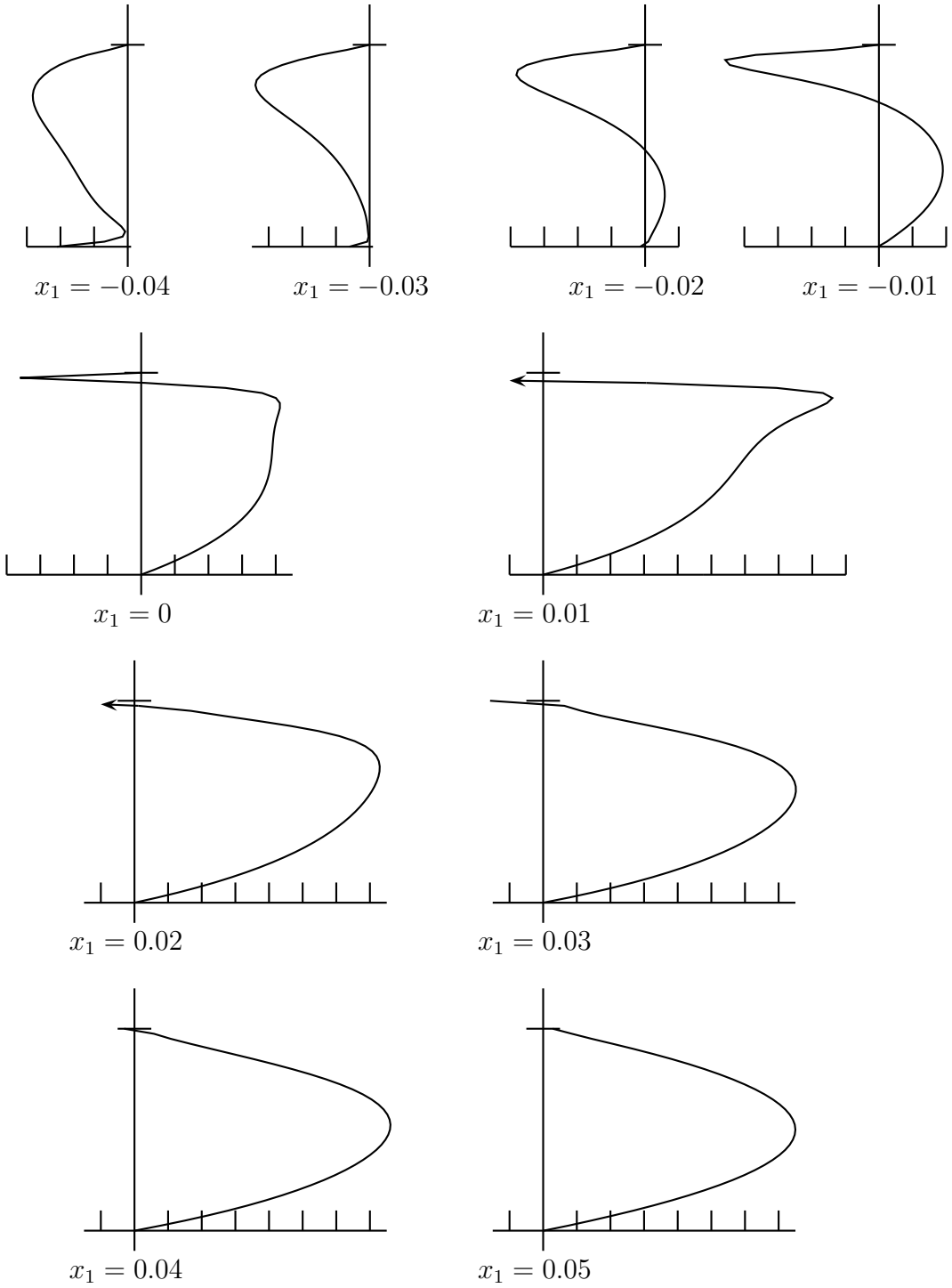

University of Pretoria etd – Labuschagne, A (2006)

7.6 Deflection

Although the main objective is to determine the stress distribution, it is of interest to compare the deflection for the two-dimensional beam with a one-dimensional model. We consider all three configurations. For both Configurations 2 and 3 we consider a built in end of length 0.1 and the free part of length 1. We take $\nu = 0.3$, $\kappa^2 = 5/6$ and $\alpha = 1200$. The deflections at $x_1 = 1$ are displayed in Table 2 for the three configurations as well as for the Timoshenko model and an accuracy of three significant digits are guaranteed for all three configurations.

Table 2: Deflections

Configuration 1	1.29
Configuration 2	1.32
Configuration 3	1.53
Timoshenko	1.29

Graphs representing these results are shown in Figure 2. Since the deflections for Configuration 1 and the Timoshenko model are the same when rounded to three significant digits, only one graph is shown.

Figure 2: Deflection comparison

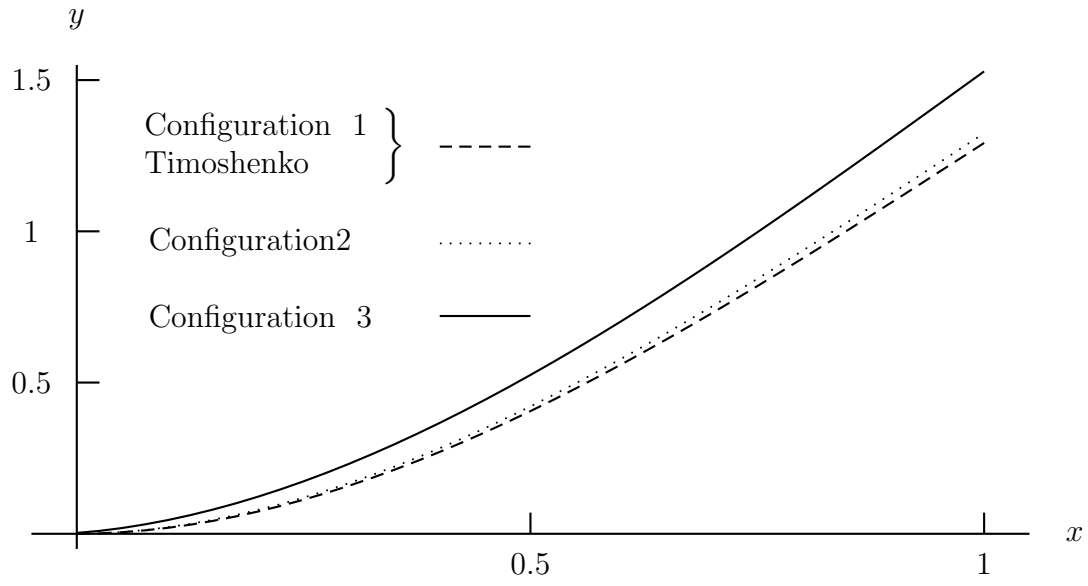

University of Pretoria etd – Labuschagne, A (2006)

The deflections of the neutral plane for Problem CTD 1 for Configurations 1 and 2 do not differ much from the deflection for the Timoshenko model, but for Configuration 3 the deflection at the endpoint is almost 20 % higher than for the Timoshenko model.

It is interesting that the Timoshenko model yields results that are so close to those obtained for Configuration 1, which is a configuration mostly used in the literature.

We are reluctant to draw any conclusion from the result. Clearly there is a need for further research and more attention should be paid to the modelling of the way the beam is built in or welded to a structure.

7.7 Eigenvalues and eigenfunctions

Eigenvalues

For the eigenvalue problem only the first two configurations are used as the third configuration gives rise to a nonlinear problem. In Table 3, the first 8 eigenvalues are compared to the corresponding eigenvalues of the cantilever Timoshenko beam and Euler-Bernoulli beam.

All the eigenvalues are given accurately to three significant digits and shown in the next table.

Table 3: Eigenvalues ($\alpha = 1200$)

Euler-Bernoulli	Timoshenko	Configuration 1	Configuration 2
$\chi_1 = 3.21 \times 10^{-2}$	$\lambda_1 = 3.16 \times 10^{-2}$	$\mu_1 = 3.17 \times 10^{-2}$	$\eta_1 = 3.06 \times 10^{-2}$
$\chi_2 = 1.26 \times 10^{0}$	$\lambda_2 = 1.14 \times 10^{0}$	$\mu_2 = 1.14 \times 10^{0}$	$\eta_2 = 1.11 \times 10^{0}$
$\chi_3 = 9.90 \times 10^{0}$	$\lambda_3 = 7.86 \times 10^{0}$	$\mu_3 = 7.72 \times 10^{0}$	$\eta_3 = 7.31 \times 10^{0}$
		$\mu_4 = 7.92 \times 10^{0}$	$\eta_4 = 7.76 \times 10^{0}$
$\chi_4 = 3.80 \times 10^{1}$	$\lambda_4 = 2.59 \times 10^{1}$	$\mu_5 = 2.62 \times 10^{1}$	$\eta_5 = 2.57 \times 10^{1}$
$\chi_5 = 1.04 \times 10^{2}$	$\lambda_5 = 5.99 \times 10^{1}$	$\mu_6 = 6.08 \times 10^{1}$	$\eta_6 = 5.99 \times 10^{1}$
		$\mu_7 = 6.93 \times 10^{1}$	$\eta_7 = 6.57 \times 10^{1}$
$\chi_6 = 2.32 \times 10^{2}$	$\lambda_6 = 1.13 \times 10^{2}$	$\mu_8 = 1.15 \times 10^{2}$	$\eta_8 = 1.14 \times 10^{2}$

The eigenvalues for the Timoshenko beam compare well with those for the two-dimensional beam except for μ_3, η_3 μ_7 and η_7. It is notable that none of

University of Pretoria etd – Labuschagne, A (2006)

the eigenvalues for the Timoshenko model are related to them. To find an explanation, we turn to the eigenfunctions.

Eigenfunctions

We used only Configuration 1 to approximate eigenfunctions for the two-dimensional model. The mode shapes for the first five eigenvalues for the Timoshenko model compare well with the mode shapes for the two-dimensional models, where the comparison is made with the vertical displacements of the neutral plane ($x_2 = 0.05$). We present one example. In Figure 3 the mode shape of the deflection of the Timoshenko model for $\lambda_3 = 7.86$ is shown, as well as the mode shape for Configuration 1 for $\mu_4 = 7.92$. These two mode shapes are the same. It is clear that μ_4 correspond to λ_3.

Now, consider the mode shape for $\mu_3 = 7.72$. The vertical displacement of the neutral plane turns out to be the zero function. We conclude that this eigenvalue corresponds to a two-dimensional effect.

Figure 3: Mode shape comparison

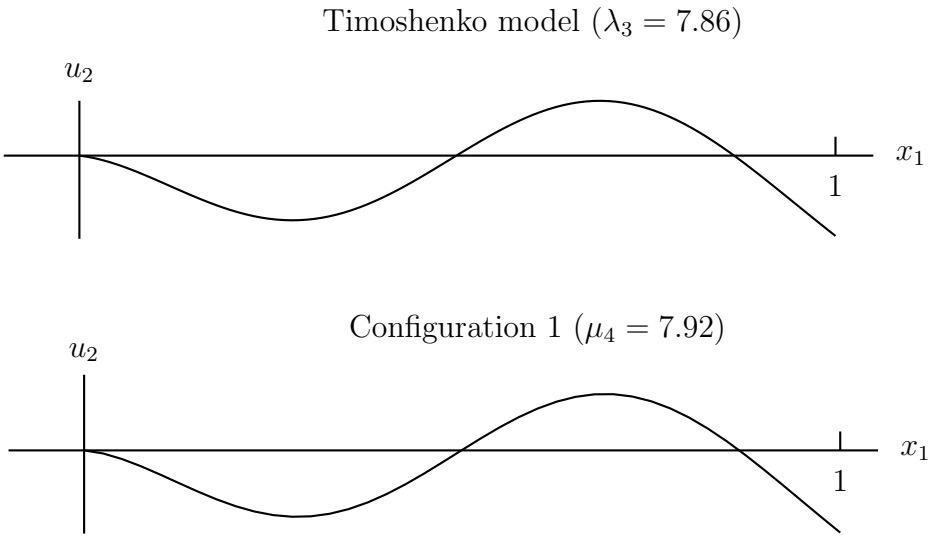

University of Pretoria etd – Labuschagne, A (2006)

Two-dimensional effects

The two-dimensional effects become visible when the displacement of the line $x_1 = 0.5$ (in the reference configuration) is examined. The Timoshenko model suggests straight lines when u_1 is plotted versus x_2 (at fixed x_1-values). The eigenvalue $\mu_4 = 7.92$ yields this result. We have a completely different result for $\mu_3 = 7.72$. The values of u_1 are almost constant (but not zero) and the line remains vertical. This implies a horizontal shift and it is clear that we have a two-dimensional effect that is not related to the one-dimensional beam theory.

The results indicate that the Timoshenko model is remarkably accurate compared to the two-dimensional model, provided that the application is one for which beam theory is intended. However, comparison to a three-dimensional model is preferable to establish the accuracy of the Timoshenko model. The conclusion is that further research needs to be done.